Metal Coordination as a Method for Templating Peptide Conformation

Zong-Qiang Tian and Paul A. Bartlett*

Contribution from the Department of Chemistry, University of California, Berkeley, California 94720-1460

Received July 24, 1995[⊗]

Abstract: The use of a metal template was explored as a strategy for controlling the conformation of a short peptide. A CAVEAT search of the Cambridge Structural Database suggested that peptide complexes of the Cu(II) ion may adopt the appropriate conformation to mimic the Trp-Arg-Tyr β-turn segment of tendamistat, a proteinaceous inhibitor of α-amylase. Complexation of tetrapeptides containing this sequence with the Cu(II) ion leads to an average enhancement of 200-fold in their ability to inhibit the enzyme. Whereas the free peptides Gly-Trp-Arg-Tyr (GWRY), Gly-Trp-Arg-D-Tyr (GWRy), and Trp-Arg-Tyr-Gly (WRYG) exhibit inhibition constants K_i^L in the range of 680 to 750 μM, those for their Cu(II) complexes, K_i^{CuL}, were found to be 2.4−5.9 μM. Since Cu(II) ion is itself a potent inhibitor of α-amylase ($K_i^{Cu} = 1$ μM), several methods were used to determine the inhibition constants of the peptide complexes. The most effective employed fixed concentrations of both Cu(II) (20 μM) and tetrapeptides (0.4−2.0 mM), with variation of the ratio of the subject tetrapeptide to a non-inhibitory tetrapeptide like tetraglycine (GGGG) or Gly-Gly-Phe-Leu (GGFL). Under these conditions, almost all of the copper ion is in the form of a peptide complex, and the concentration of the inhibitory complex itself is determined by the mole ratio of the peptides and their complexation constants, *K*. Nonlinear regression analysis of the data allowed consistent values of K_i^{CuL} as well as *K* to be determined for each peptide. The large enhancement in affinity induced by copper complexation suggests that the metal ion templates the peptides and increases the proportion present in the bioactive β-turn conformation.

A key strategy in the design of peptidomimetics is conformational constraint, either through replacement of the peptide backbone with rigid, cyclic structures,[1−4] or through macrocyclization, in which the backbone is retained but flexibility is reduced by bridging the side chains and/or the main chain.[5−15] While most examples of this strategy involve covalent bonding in the backbone template or in the bridging unit, in a few instances metal-ion coordination has been employed to link modified amino acid side chains or to induce a specific conformation in a template.[16−19] An advantage of this approach is the ease with which templated or macrocyclic structures can be formed by metal complexation (Figure 1), in contrast to designs that require multistep synthetic routes to covalently linked structures.

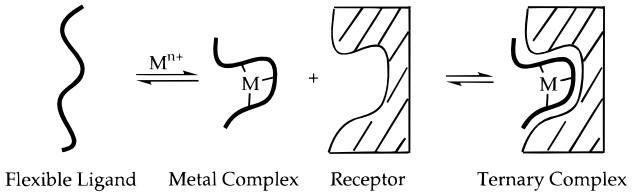

Figure 1. Conformational restriction via metal complexation in structure-based design.

The design of peptidomimetics has played an important role in the development of structure-based design principles, since it is frequently for peptidic ligands that structural information is available from crystallography or NMR, and in some cases for receptor binding sites which are specific for peptides (e.g., proteases).[20−23] One strategy for the design of peptidomimetics entails the identification of a core structure (template) that can orient substituents (side chains) in a specific vector relationship, in order to position functional groups or recognition elements

[⊗] Abstract published in *Advance ACS Abstracts,* December 15, 1995.

(1) Hinds, M. G.; Richards, N. G. J.; Robinson, J. A. *J. Chem. Soc., Chem. Commun.* **1988**, 1447−1449.
(2) Nagai, U.; Sato, K.; Nakamura, R.; Kato, R. *Tetrahedron* **1993**, *49*, 3577−3592.
(3) Smith, A. B., III; Guzman, M. C.; Sprengeler, P. A.; Keenan, T. P.; Holcomb, R. C.; Wood, J. L.; Carroll, P. J.; Hirschmann, R. *J. Am. Chem. Soc.* **1994**, *116*, 9947−9962.
(4) Su, T.; Nakanishi, H.; Xue, L.; Chen, B.; Tuladhar, S.; Johnson, M. E.; Kahn, M. *Bioorg. Med. Chem. Lett.* **1993**, *3*, 835−840.
(5) Cheng, S.; Craig, W. S.; Mullen, D.; Tschopp, J. F.; Dixon, D.; Pierschbacher, M. D. *J. Med. Chem.* **1994**, *37*, 1−8.
(6) Etzkorn, F. A.; Guo, T.; Lipton, M. A.; Goldberg, S. D.; Bartlett, P. A. *J. Am. Chem. Soc.* **1994**, *116*, 10412−10425.
(7) Hruby, V. J.; Al-Obeidi, F.; Kazmierski, W. *Biochem. J.* **1990**, *268*, 249−262.
(8) Jackson, S.; DeGrado, W. F.; Dwivedi, A.; Parthasarathy, A.; Higley, A.; Krywko, J.; Rockwell, A.; Markwalder, J.; Wells, G.; Wexler, R.; Mousa, S.; Harlow, R. L. *J. Am. Chem. Soc.* **1994**, *116*, 3220−3230.
(9) Kopple, K. D.; Baures, P. W.; Bean, J. W.; D'Ambrosio, C. A.; Hughes, J. L.; Peishoff, C. E.; Eggleston, D. S. *J. Am. Chem. Soc.* **1992**, *114*, 9615−9623.
(10) Matter, H.; Kessler, H. *J. Am. Chem. Soc.* **1995**, *117*, 3347−3359.
(11) McDowell, R. S.; Gadek, T. R. *J. Am. Chem. Soc.* **1992**, *114*, 9245−9253.
(12) Morgan, B. P.; Bartlett, P. A.; Holland, D. R.; Matthews, B. W. *J. Am. Chem. Soc.* **1994**, *116*, 3251−3260.
(13) Podlogar, B. L.; Farr, R. A.; Friedrich, D.; Tarnus, C.; Huber, E. W.; Cregge, R. J.; Schirlin, D. *J. Med. Chem.* **1994**, *37*, 3684−3692.
(14) Struthers, R. S.; Tanaka, G.; Koerber, S. C.; Solmajer, T.; Baniak, E. L.; Gierasch, L. M.; Vale, W.; Rivier, J.; Hagler, A. T. *Proteins* **1990**, *8*, 295−304.
(15) Yang, L.; Weber, A. E.; Greenlee, W. J.; Patchett, A. A. *Tetrahedron Lett.* **1993**, *34*, 7035−7038.
(16) Ghadiri, M. R.; Fernholz, A. K. *J. Am. Chem. Soc.* **1990**, *112*, 9633−9635.
(17) Ghadiri, M. R.; Choi, C. *J. Am. Chem. Soc.* **1990**, *112*, 1630−1632.
(18) Schneider, J. P.; Kelly, J. W. *J. Am. Chem. Soc.* **1995**, *117*, 2533−2546.
(19) Ruan, F.; Chen, Y.; Hopkins, P. B. *J. Am. Chem. Soc.* **1990**, *112*, 9403−9404.
(20) Appelt, K.; et al. *J. Med. Chem.* **1991**, *34*, 1925−1934.
(21) Kuntz, I. D.; Meng, E. C.; Shoichet, B. K. *Acc. Chem. Res.* **1994**, *27*, 117−123.
(22) Lam, P. Y. S.; et al. *Science* **1994**, *263*, 380−384.
(23) Verlinde, C. L.; Hol, W. G. *Structure* **1994**, *2*, 577−587.

0002-7863/96/1518-0943$12.00/0

correctly in three dimensions. The program CAVEAT was devised to facilitate this approach by identifying structures or fragments from 3-D databases that could serve as such cores.[24] We have described the origination and implementation of this approach in connection with the design of **1**, an inhibitor of α-amylase believed to function as a mimic of the proteinaceous inhibitor tendamistat.[6,10] The cyclic hexapeptide orients the triad of Trp-Arg-Tyr around a β-turn in a fashion similar to the protein,[25,26] for which these residues are central to the binding interaction.[27] We now describe the use of CAVEAT to identify potential templates for the tendamistat β-turn from a database of metal complexes, the design of metal−peptide complexes as conformationally constrained derivatives, and the effect of metal complexation on the binding affinity of these peptides.

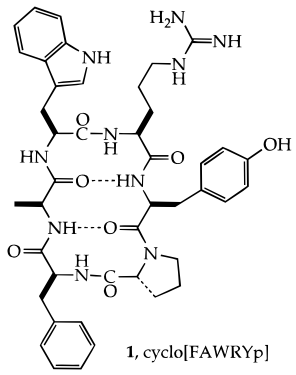

1, cyclo[FAWRYp]

As outlined previously,[6] the $C_\alpha-C_\beta$ bonds of the ^{18}Trp-^{19}Arg-^{20}Tyr triad of tendamistat (Figure 2a) were used as the query vectors for a CAVEAT search of the Cambridge Structural Database (CSD).[28] The hits identified from this search were screened further with the program CLASS,[24] and only those structures with metals as part of the core ring system were retained. A representative set of hits is shown in Figure 3 and includes both acyclic as well as macrocyclic metal ligands. The most attractive class of complexes are those in which a peptide itself serves as the complexing agent, through the peptide backbone. For example, the complex of Cu(II) with pentaglycine, **2**,[29] overlaps closely with the β-turn residues of

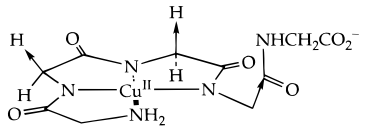

2, Gly_5·Cu; matching bonds indicated

tendamistat, with the *pro-S* hydrogens of the 2nd and 3rd residues and the Cα-to-carbonyl bond of the 4th residue matching the CAVEAT search vectors, as shown in Figure 2b. We therefore proposed the copper complexes of Gly-Trp-Arg-Tyr (GWRY) and Gly-Trp-Arg-D-Tyr (GWRy) as our targets. Square planar coordination of Cu(II) to the N-terminal amino group and the amide nitrogen atoms (in the deprotonated form) offered a simple way to restrict the conformation of the peptides and orient the side chains as they are in tendamistat. Both configurations of the terminal tyrosine residue were explored because it was not clear which conformation would be preferred by the uncoordinated carboxylate. The analogous tetrapeptides Gly-Trp-Orn-Tyr (GWOY) and Trp-Arg-Tyr-Gly (WRYG) were also studied as comparison compounds.

Results

Porcine pancreatic α-amylase was assayed with *p*-nitrophenyl maltotrioside (*p*-NPG_3) as substrate in 2-hydroxyethyl-1,4-piperizineethanesulfonic acid (HEPES) buffer at pH 7,[6] and inhibition was determined for various combinations of peptides and cupric ions. The absorbance change caused by Cu(II) at the assay wavelength of 405 nm is negligible at the micromolar concentrations used. However, this ion is a potent inhibitor of α-amylase, with a K_i value of 1.0 ± 0.3 μM (K_i^{Cu}) as determined by Dixon analysis (eq 1).[30] A common intercept on the 1/*V* axis for reciprocal plots of 1/*V* vs 1/*S* at various $CuCl_2$ concentrations indicates that the Cu(II) ion is primarily a competitive inhibitor for α-amylase. The tetrapeptides by themselves are weak inhibitors of the enzyme, with K_i values (K_i^L) from 0.68−0.75 mM for those containing arginine to 2.5 mM for the ornithine analog (Table 1). These inhibition constants are comparable to those determined for other acyclic peptides containing the WRY sequence.[6]

$$\frac{V_0}{V_i} = 1 + \frac{[I]}{(1 + [S]/K_m)K_i} \qquad (1)$$

Although the ease with which Cu(II)−peptide complexes like **2** can be prepared is an advantage of this strategy, a disadvantage is the rapid equilibrium between complexed and uncomplexed states for the ligand.[31,32] As a consequence, the usual bimolecular ligand−receptor equilibrium becomes a termolecular metal−ligand−receptor system (Figure 1). Thus, the K_i values for these complexes (K_i^{CuL}) cannot be measured directly, because free Cu(II) ion, free peptide, and the Cu(II)−peptide complex are all present and all three species inhibit. With the assumption that they inhibit competitively, the initial rate can be expressed in eq 2 and its reciprocal, eq 3.

$$V = \frac{V_{max}[S]}{[S] + K_m\left(1 + \frac{[Cu^{2+}]}{K_i^{Cu}} + \frac{[L]}{K_i^{L}} + \frac{[CuL]}{K_i^{CuL}}\right)} \qquad (2)$$

$$\frac{1}{V} = \frac{1}{V_{max}} + \frac{K_m}{V_{max}[S]}\left(1 + \frac{[Cu^{2+}]}{K_i^{Cu}} + \frac{[L]}{K_i^{L}} + \frac{[CuL]}{K_i^{CuL}}\right) \qquad (3)$$

The equilibrium for Cu(II)−peptide formation is reflected in eq 4, in which Cu^{2+} represents all forms of copper ion not bound to the peptide, L represents the peptide ligand, and CuL represents all forms of the Cu(II)−peptide complex, with association constant $K = [CuL]/[Cu^{2+}][L]$. When the total ligand concentration is in large excess of the total Cu(II) concentration ($[L]_0 \gg [Cu^{2+}]_0$), then $[L] \approx [L]_0$; moreover, if $K[L]_0 \gg 1$, then $[CuL] \approx [Cu^{2+}]_0$ and $[Cu^{2+}] \approx [Cu^{2+}]_0/K[L]_0$.

$$Cu^{2+} + L \rightleftharpoons CuL \qquad (4)$$

(24) Lauri, G.; Bartlett, P. A. *J. Comp. Aided Mol. Design* **1994**, *8*, 51−66.
(25) Kline, A. D.; Braun, W.; Wüthrich, K. *J. Mol. Biol.* **1986**, *189*, 367−382.
(26) Pflugrath, J. W.; Wiegand, G.; Huber, R.; Vértesy, L. *J. Mol. Biol.* **1986**, *189*, 383−386.
(27) Wiegand, G.; Epp, O.; Huber, R. *J. Mol. Biol.* **1995**, *247*, 99−110.
(28) Allen, F. H.; Kennard, O.; Taylor, R. *Acc. Chem. Res.* **1983**, *16*, 146−153.
(29) Blount, J. F.; Freeman, H. C.; Holland, R. V.; Milburn, G. H. W. *J. Biol. Chem.* **1970**, *245*, 5177−5185.
(30) Segel, I. H. *Enzyme Kinetics*; Wiley-Interscience: New York, 1975.
(31) Margerum, D. W.; Dukes, G. R. *Met. Ions Biol. Syst.* **1974**, *1*, 157−212.
(32) Sigel, H.; Martin, R. B. *Chem. Rev.* **1982**, *82*, 385−426.

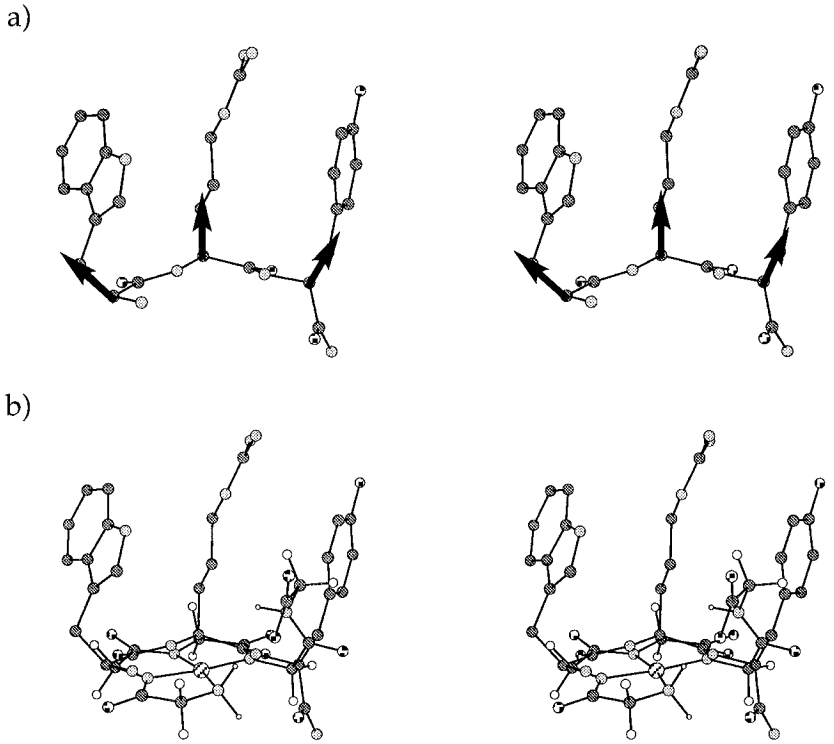

Figure 2. (a) The vectors defined by the $C_\alpha - C_\beta$ bonds of the ^{18}Trp-^{19}Arg-^{20}Tyr β-turn of tendamistat. (b) Superposition of the β-turn and the Cu(II) complex of pentaglycine.

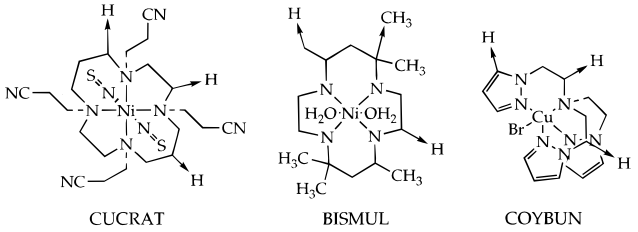

Figure 3. Examples of metal complexes and the bonds that match the CAVEAT vectors of Figure 2a.

Table 1. Inhibition of α-Amylase by Peptides and Their Copper(II) Complexes[a]

inhibitor	K_i^L (μM)	K_i^{CuL} (μM)	K^{CuL} (mM^{-1})
WRY	520[b]	>100[c]	*c*
Ac-FSWRYp-NH2	320[b]	*d*	*d*
cyclo[FSWRYp]	14[b]	*d*	*d*
Cu^{2+}	1.0		
GGGG	>2500	113 ± 14	64 ± 1
GGFL	>2000	56 ± 8	65 ± 3
GWOY	2500 ± 500	15 ± 3	226 ± 15
WRYG	740 ± 30	5.9 ± 0.6	169 ± 19
GWRY	750 ± 50	4.7 ± 0.6	135 ± 8
GWRy	680 ± 20	2.4 ± 0.3	145 ± 16

[a] Determined at pH 7.0; K_i^L = inhibition constant of free peptide; K_i^{CuL} = inhibition constant of the Cu(II)−peptide complex; K^{CuL} = association constant of the Cu(II)−peptide complex. [b] From Etzkorn et al.[6] [c] Cu(II) complexation with tripeptide WRY did not increase its inhibitory potency significantly, and only an approximate measure of K_i^{CuL} could be obtained. [d] Not determined.

Non-inhibitory Peptides. For a nonbinding peptide such as tetraglycine (GGGG), which shows no inhibition of α-amylase up to 2.5 mM, K can be determined indirectly by measuring the decrease of Cu(II) inhibition resulting from GGGG coordination. For a given set of experiments, [GGGG] was kept constant and in large excess of [$CuCl_2$], which was varied. Under these conditions, the initial rate can be expressed in eq 5 and the general equation for Dixon analysis (eq 1) can be adapted to obtain an apparent inhibition constant K_{iapp} (eq 6 and Figure 4a). The dependence of K_{iapp} on [L] is expressed in eq 7; the plot of $1/K_{iapp}$ vs 1/[L] shows a good linear relationship (Figure 4b), giving the association constant (K = 64 mM^{-1}) from the slope, as well as the average inhibition constant for all forms of the metal complex, K_i^{CuL} = 113 μM, from the intercept (Table 1). Treatment of the experimental data assuming that the copper complex Cu(GGGG) does not inhibit gives inconsistent results.

$$\frac{1}{V} = \frac{1}{V_{max}} + \frac{K_m}{V_{max}[S]}\left(1 + \frac{[Cu^{2+}]}{K_i^{Cu}} + \frac{[CuL]}{K_i^{CuL}}\right) \quad (5)$$

$$\frac{V_0^L}{V_i} = 1 + \frac{[CuCl_2]}{1 + [S]/K_m}\left(\frac{1}{K_{iapp}}\right) \quad (6)$$

$$\frac{1}{K_{iapp}} = \frac{1}{K_i^{Cu}K[L]} + \frac{1}{K_i^{CuL}} \quad (7)$$

The same analysis was performed with Gly-Gly-Phe-Leu (GGFL), which also shows no inhibition of α-amylase up to 2 mM but resembles GWRY and GWOY sterically better than GGGG does. A similar value was obtained for the association constant K (Table 1), validating the assumption that $K[L]_0 \gg 1$ at the mM concentrations of peptides used.

Inhibitory Peptides. For the Arg- and Orn-containing peptides, all three species in eq 4 are inhibitors. We took two different approaches to elucidate the K_i values for their Cu(II)−peptide complexes: (A) studying a given concentration of the peptide L, while varying the concentration of Cu(II), and (B) studying a given concentration of total peptide and Cu(II), while varying the ratio of the inhibitory peptide L to a non-inhibitory peptide such as GGGG.

For method A, with $[L]_0 \gg [CuCl_2]$, the rate equation (eq 3) is adapted to give eq 8. The reference rate V_0^L, obtained with the same concentration of peptide in the absence of copper ion,

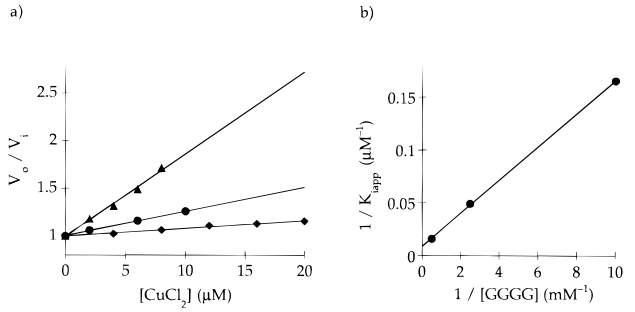

Figure 4. (a) Dixon plot for the inhibition of α-amylase by $CuCl_2$ in the presence of excess GGGG; V_0 for each concentration of peptide is the initial rate in the presence of peptide and the absence of $CuCl_2$. [GGGG] = 0.1 mM (▲), 0.4 mM (●), and 2.0 mM (◆). (b) Plot of $1/K_{iapp}$ vs 1/[L] (eq 7) for GGGG.

is described by eq 9, which can be combined with eq 8 to give eq 10. In this case the slope of the Dixon plot (V_0^L/V_i vs $[CuCl_2]$) has a complex, non-linear dependence on [L] (eq 11; plots for GWRy shown in Figure 5). Our attempts to obtain both K and K_i^{CuL} by nonlinear regression of the data for slope vs [L] for the inhibitory peptides were not successful. The value for K was thus assigned as 64 ± 3 mM^{-1} (average value measured for GGGG and GGFL) in order to calculate a value for K_i^{CuL} from the slope of the Dixon plot for each concentration of peptide. The K_i^{CuL} values calculated in this way for the Cu(II)−peptide complexes are listed in Table 2.

$$\frac{1}{V} = \frac{1}{V_{max}} + \frac{K_m}{V_{max}[S]}\left(1 + \frac{[CuCl_2]}{K_i^{Cu}K[L]} + \frac{[L]}{K_i^{L}} + \frac{[CuCl_2]}{K_i^{CuL}}\right) \quad (8)$$

$$\frac{1}{V_0^L} = \frac{1}{V_{max}} + \frac{K_m}{V_{max}[S]}\left(1 + \frac{[L]}{K_i^{L}}\right) \quad (9)$$

$$\frac{V_0^L}{V_i} = 1 + \frac{[CuCl_2]}{1 + [S]/K_m + [L]/K_i^{L}}\left(\frac{1}{K_i^{Cu}K[L]} + \frac{1}{K_i^{CuL}}\right) \quad (10)$$

$$\text{slope} = \frac{1/K_i^{CuL} + 1/K_i^{Cu}K[L]}{1 + [S]/K_m + [L]/K_i^{L}} \quad (11)$$

Although the average values for K_i^{CuL} give an indication of the affinities of these complexes for α-amylase, it is clear that analytical method A suffers from a systematic error. In this method, the concentration of the two most potently inhibiting species, free Cu^{2+} ion and the Cu(II)−peptide complex, vary together, while the concentration of the weakly inhibiting, free peptide is fixed. As a result, it is difficult to separate the inhibitory contributions from the two strong inhibitors. For method B, the sum of the concentrations of the binding (L) and nonbinding (GGGG) tetrapeptides is kept constant and in large excess of a fixed concentration of copper ion (20 μM). As a result, it is the concentration of free L that is varied along with that of the CuL complex, not that of the copper ion. We expected method B to provide more accurate results because inhibition by copper ion is suppressed by complexation to free peptides, and inhibition due to the CuL complex can be separated more easily from that due to the free peptide.

In our first analysis according to method B, we made the simplifying assumption that all the tetrapeptides studied bind Cu(II) with the same association constant K, and thus that the ratio of the CuL and Cu(GGGG) complexes would be equal to the ratio of their total concentrations. Moreover, since the total concentration ($[L]_T$) of the two peptides is in large excess of the concentration of $CuCl_2$, almost all of the Cu(II) ion is complexed, and the following relationships hold (eqs 12−15):

$$[CuL] + [Cu(GGGG)] \approx [CuCl_2] \quad (12)$$

$$[CuL] \cong \frac{[CuCl_2][L]}{[L]_T} \quad (13)$$

$$[Cu(GGGG)] \cong \frac{[CuCl_2][GGGG]}{[L]_T} = \frac{[CuCl_2]([L]_T - [L])}{[L]_T} \quad (14)$$

$$[Cu^{2+}] \cong \frac{[CuCl_2]}{K[L]_T} \quad (15)$$

The rate expression (eq 16) for the four-inhibitor system (Cu^{2+}, Cu(GGGG), L, and CuL) can thus be adapted to give eq 17. Using the rate obtained with $CuCl_2$ and GGGG alone ([L] = 0) as the reference V_0 (eq 18), eq 19 can be derived. Values calculated for K_i^{CuL} by this method are comparable to those determined by method A, but curved Dixon plots (those for GWRy and GWRY are depicted in Figure 6) still showed evidence of an uncontrolled variable.

$$\frac{1}{V} = \frac{1}{V_{max}} + \frac{K_m}{V_{max}[S]}\left(1 + \frac{[Cu^{2+}]}{K_i^{Cu}} + \frac{[L]}{K_i^{L}} + \frac{[CuL]}{K_i^{CuL}} + \frac{[Cu(GGGG)]}{K_i^{Cu(GGGG)}}\right) \quad (16)$$

$$\frac{1}{V} = \frac{1}{V_{max}} + \frac{K_m}{V_{max}[S]}\left(1 + \frac{[CuCl_2]}{K_i^{Cu}K[L]_T} + \frac{[L]}{K_i^{L}} + \frac{[CuCl_2][L]}{K_i^{CuL}[L]_T} + \frac{[CuCl_2]([L]_T - [L])}{K_i^{Cu(GGGG)}[L]_T}\right) \quad (17)$$

$$\frac{1}{V_0} = \frac{1}{V_{max}} + \frac{K_m}{V_{max}[S]}\left(1 + \frac{[CuCl_2]}{K_i^{Cu}K[L]_T} + \frac{[CuCl_2]}{K_i^{Cu(GGGG)}}\right) \quad (18)$$

$$\frac{V_0}{V_i} = 1 + \frac{\frac{[L]}{K_i^{L}} + \frac{[CuCl_2][L]}{[L]_T}\left(\frac{1}{K_i^{CuL}} - \frac{1}{K_i^{Cu(GGGG)}}\right)}{1 + \frac{[S]}{K_m} + [CuCl_2]\left(\frac{1}{K_i^{Cu}K[L]_T} + \frac{1}{K_i^{Cu(GGGG)}}\right)} \quad (19)$$

This curvature arises from the assumption that Cu(GGGG) and the other CuL complexes have the same association constants; therefore, we allowed for this difference in our complete analysis according to method B. If the association constant for CuL ($K^{CuL} = [CuL]/[Cu^{2+}][L]$) is expressed as αK, where K is the association constant of tetraglycine ($K^{Cu(GGGG)} = [Cu(GGGG)]/[Cu^{2+}][GGGG]$), eqs 13−15 become eqs 20−22:

$$[CuL] \cong \frac{[CuCl_2]\alpha[L]}{[L]_T + (\alpha - 1)[L]} \quad (20)$$

$$[Cu(GGGG)] \cong \frac{[CuCl_2]([L]_T - [L])}{[L]_T + (\alpha - 1)[L]} \quad (21)$$

Table 2. Inhibition Constants for Cu(II)−Peptide Complexes Determined by Method A

	GWOY			WRYG			GWRY			GWRy		
[L] (mM)	slope (mM^{-1})[a]	K_i^{CuL} (μM)[b,c]		slope	K_i^{CuL}		slope	K_i^{CuL}		slope	K_i^{CuL}	
0.1	0.077(2)		9.4				0.142(8)	7.5	4.6			
0.2	0.066(1)	19	9.2				0.130(1)	4.0	4.1			
0.3	0.543(3)	17	10.5									
0.4	0.046(3)	18	12.0	0.088(3)	5.6	5.0	0.097(4)	5.1	4.6	0.202(2)	2.2	2.1
0.6	0.046(2)	14	10.9				0.091(3)	4.5	4.3			
0.8	0.044(1)	13	10.8									
1.0	0.047(1)	11	9.7	0.052(1)	6.5	6.1	0.090(9)	3.6	3.5	0.132(7)	2.4	2.4
2.0	0.047(1)	8	8.0	0.327(1)	7.0	6.8	0.088(3)	2.5	2.5	0.093(4)	2.4	2.4
av[c]		**14 ± 4**	**10 ± 1**		**6.4 ± 0.7**	**6.0 ± 0.9**		**5 ± 2**	**3.9 ± 0.8**		**2.3 ± 0.1**	**2.3 ± 0.2**

[a] Slope from Dixon plots (eq 10, Figure 5); the number in parentheses is the error in the last digit, from the standard deviation of the linear regression. [b] K_i^{CuL} values calculated using eq 11, with $K_m = 1.1$ mM, $K_i^{Cu} = 1.0$ μM, $K_i^{GWOY} = 2.5$ mM, $K_i^{WRYG} = 0.74$ mM, $K_i^{GWRY} = 0.75$ mM, and $K_i^{GWRy} = 0.68$ mM. [c] The K_i^{CuL} values in the first column were determined using $K^{CuL} = 64$ mM^{-1} for all tetrapeptides; the values in the second column were calculated with $K^{Cu(GWOY)} = 226$ mM^{-1}, $K^{Cu(WRYG)} = 169$ mM^{-1}, $K^{Cu(GWRY)} = 135$ mM^{-1}, and $K^{Cu(GWRy)} = 145$ mM^{-1}.

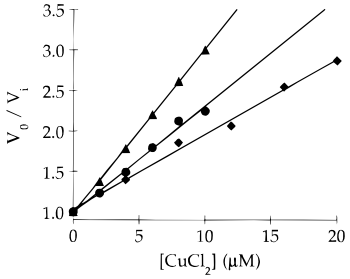

Figure 5. Dixon plot for inhibition of α-amylase by $CuCl_2$ in the presence of excess GWRy; V_0 for each concentration of peptide is the initial rate in the presence of peptide and the absence of $CuCl_2$. [GWRy] = 0.4 mM (▲), 1.0 mM (●), and 2.0 mM (◆).

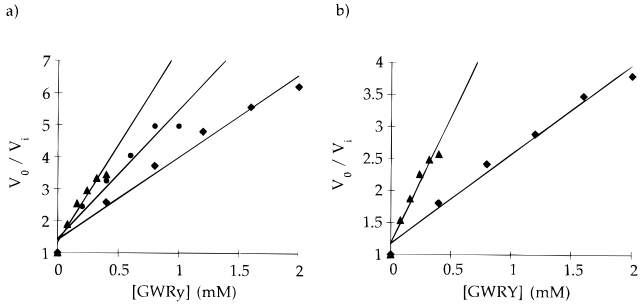

Figure 6. Dixon plots for inhibition of α-amylase by (a) GWRy and (b) GWRY in the presence of 20 μM $CuCl_2$ and GGGG, with the total ligand concentration ($[L]_T$) fixed (method B); experimental data fit to eq 19. V_0 is the initial rate for reaction in the presence of $CuCl_2$ and GGGG alone. $[L]_T = 0.4$ mM (▲), 1.0 mM (●), and 2.0 mM (◆).

$$[Cu^{2+}] \cong \frac{[CuCl_2]}{K([L]_T + (\alpha - 1)[L])} \tag{22}$$

Although eqs 16 and 18 remain valid expressions for V_i and V_0, respectively, V_0/V_i has a nonlinear dependence on [L] (eq 23). Providing independently-determined values for K_m, K_i^L, K_i^{Cu}, $K_i^{Cu(GGGG)}$, and K, nonlinear regression of the data for V_0/V_i vs [L] allows values for K_i^{CuL} as well as α to be calculated for each of the binding peptides (Table 3); initial values for the nonlinear regression analysis were chosen from simple linear analysis. The plots for GWRy and GWRY are shown in Figure 7 and demonstrate that the more comprehensive analysis reproduces the experimental behavior quite well. The inhibition constants calculated are 2.4 ± 0.3 μM for $K_i^{Cu(GWRy)}$, 4.7 ± 0.6 μM for $K_i^{Cu(GWRY)}$, 15 ± 3 μM for $K_i^{Cu(GWOY)}$, and 5.9 ± 0.6 μM for $K_i^{Cu(WRYG)}$, with the values for α of 2.3 ± 0.3, 2.1 ± 0.1, 3.5 ± 0.2, and 2.6 ± 0.3, respectively.

$$\frac{V_0}{V_i} = 1 + \frac{\dfrac{[L]}{K_i^L} + \dfrac{[CuCl_2][L]}{[L]_T + (\alpha - 1)[L]}\left\{\dfrac{1 - \alpha}{K_i^{Cu} K [L]_T} + \alpha\left(\dfrac{1}{K_i^{CuL}} - \dfrac{1}{K_i^{Cu(GGGG)}}\right)\right\}}{1 + \dfrac{[S]}{K_m} + [CuCl_2]\left(\dfrac{1}{K_i^{Cu} K [L]_T} + \dfrac{1}{K_i^{Cu(GGGG)}}\right)} \tag{23}$$

The association constants K^{CuL} for the peptide−Cu(II) complexes can be calculated from the values determined for α (Table 3) and then used to reanalyze the results from method A. The values calculated in this manner for K_i^{CuL} show smaller variances with respect to [L] for Cu(GWOY) and Cu(GWRY) (Table 2). Comparable values for the inhibition constants were obtained from the two methods of analysis, with or without the simplifying assumptions, although the data are best modeled by method B with full analysis of the variables.

As inhibitors of α-amylase, the Cu(II)−peptide complexes compare favorably with the tendamistat mimics reported previously, in which the Trp-Arg-Tyr triad is constrained in the β-turn conformation by incorporation in the framework of a cyclic hexapeptide.[6,10] In comparison to the unconstrained acyclic peptides, the copper complexes are improved more than two orders of magnitude in affinity, in spite of the fact that more than one form is likely to be present in the equilibrium mixture (see below). By this criterion, the complexation strategy was more effective as a strategy for generating a conformationally constrained mimic of tendamistat than the covalent macrocyclization design.

The Metal−Peptide Complexation Equilibria

Deprotonation of an amide nitrogen in aqueous media in the absence of metal ion requires strongly basic conditions ($pK_a \sim 15$). However, coordination of transition metal ions increases the acidity of the amide nitrogens by stabilization of the deprotonated form.[32] The magnitude of this effect depends on the metal ion, but it can be remarkable when a five-membered chelate ring is formed.[33] The four major forms of the Cu(II)−GGGG complex in solution (Figure 8) are related by the equilibria shown in eqs 24−26 involving deprotonation of the amide NH's. The values of log K_1^H, log K_2^H, and log K_3^H in aqueous solution (ionic strength of 0.1 M) measured by

(33) Kim, M. K.; Martell, A. E. *J. Am. Chem. Soc.* **1966**, *88*, 914−918.

Table 3. Inhibition and Association Constants for Cu(II)−Peptide Complexes Determined by Method B[a]

	GWOY		WRYG		GWRY		GWRy	
[ligand]T (mM)	α	K_i^{CuL} (μM)[b]	α	K_i^{CuL}	α	K_i^{CuL}	α	K_i^{CuL}
0.4	3.7(6)	12.4(2)	3.0(2)	6.49(6)	2.2(3)	4.24(8)	2.5(2)	2.75(4)
1.0			2.6(2)	5.67(6)			2.3(4)	2.27(9)
2.0	3.4(4)	16.6(2)	2.4(5)	5.4(2)	2.0(2)	5.1(1)	2.02(8)	2.20(2)
average	3.5 ± 0.2	$\mathbf{15 \pm 3}$	2.6 ± 0.3	$\mathbf{5.9 \pm 0.6}$	2.1 ± 0.1	$\mathbf{4.7 \pm 0.6}$	2.3 ± 0.3	$\mathbf{2.4 \pm 0.3}$
K^{CuL} (mM^{-1})[b]	$\mathbf{226 \pm 15}$		$\mathbf{169 \pm 19}$		$\mathbf{135 \pm 8}$		$\mathbf{145 \pm 16}$	

[a] The values for α and K_i^{CuL} were obtained by fitting the experimental data to eq 23, with $K_i^{Cu(GGGG)} = 110\ \mu M$ and other values given in footnote *b*, Table 2. The number in parentheses is the error of the last digit, from the standard deviation of the nonlinear regression; the *R* value is >0.995 for all regressions. [b] $K^{CuL} = \alpha K^{Cu(GGGG)}$, $K^{Cu(GGGG)} = 64\ mM^{-1}$.

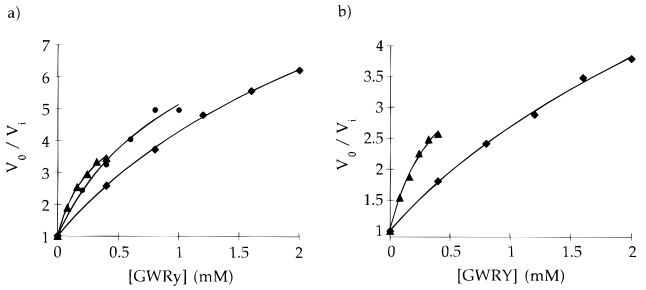

Figure 7. Experimental data from Figure 6 fit to eq 23.

potentiometric methods are 5.4, 6.8, and 9.1, respectively.[34] Using these constants, it is possible to deduce the formation constant of each species at a given [H^+]. At the assay pH of 7, the most abundant species in aqueous solution is Cu(H_{-2}L) (∼50%), followed by Cu(H_{-1}L) (∼30%). The total association constant (*K* in eq 4) estimated at pH 7 is $2 \times 10^6\ M^{-1}$. Under conditions for the α-amylase assays, 25 mM of HEPES and >30 mM of chloride ions are present as competing ligands,[35] which explain why the observed association constant is ca. 30-fold lower ($6 \times 10^4\ M^{-1}$; Table 1).

$$\mathrm{CuL} \rightleftharpoons \mathrm{Cu(H_{-1}L)} + \mathrm{H^+} \qquad K_1^{H} = \frac{[\mathrm{CuL}]}{[\mathrm{Cu(H_{-1}L)}][\mathrm{H^+}]} \tag{24}$$

$$\mathrm{Cu(H_{-1}L)} \rightleftharpoons \mathrm{Cu(H_{-2}L)} + \mathrm{H^+} \qquad K_2^{H} = \frac{[\mathrm{Cu(H_{-1}L)}]}{[\mathrm{Cu(H_{-2}L)}][\mathrm{H^+}]} \tag{25}$$

$$\mathrm{Cu(H_{-2}L)} \rightleftharpoons \mathrm{Cu(H_{-3}L)} + \mathrm{H^+} \qquad K_3^{H} = \frac{[\mathrm{Cu(H_{-2}L)}]}{[\mathrm{Cu(H_{-3}L)}][\mathrm{H^+}]} \tag{26}$$

Amino acids with potentially coordinating side chains such as arginine, lysine, and ornithine nonetheless behave primarily as bidentate ligands toward Cu(II), through the α-amino group and a carboxylate oxygen.[35−37] Moreover, dipeptides containing arginine coordinate to Cu(II) through the peptide backbone, in similar fashion to the corresponding leucine analogs.[38,39] The inhibitory peptides therefore are likely to coordinate to Cu(II) as GGGG and GGFL do, and the major form of Cu(GWXY) (X = R, O) and Cu(GWRy) should also be Cu(H_{-2}L) and

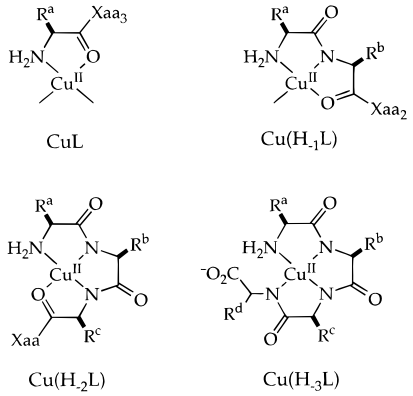

Figure 8. Four possible forms of the Cu(II)−tetrapeptide complexes in solution; Cu(H_{-1}L) and Cu(H_{-2}L) are expected to be the major species at pH 7.

Cu(H_{-1}L), as shown in Figure 8. Although Cu(H_{-3}L), the species which corresponds to the original CAVEAT hit, is not the major component of the equilibrium at neutral pH, it may be favored on binding to α-amylase. In the absence of structural information on the bound form of the peptide−copper complex, we cannot exclude the possibility that the copper is coordinated to an active site residue in addition to the peptide, which would result in a ternary complex quite different from that originally envisaged.

Conclusions

As a general approach to conformationally constrained peptides, metal coordination has its advantages and disadvantages. It is a relatively unexplored strategy which has seen little application in the design of enzyme inhibitors.[40] It has the advantage, as pointed out in the introduction, that the synthesis required is relatively short, and in spite of the complexity of the analyses described, initial results may be obtained rapidly. Enhanced affinity of a metal−peptide complex for a receptor target may provide some insight into the conformation that the peptide adopts on binding, and thus suggests alternative, covalent designs for a peptidomimetic. This strategy may also offer a novel method for producing heavy ion derivatives for solving the crystal structure of the enzyme−inhibitor complex. However, the approach has its limitations. From a design perspective, there is a paucity of force field parameters for modeling such metal complexes. As shown in the present case, unless exchange-inert metals are employed, the assay can be complicated by the equilibrium nature of the association process, as well as by direct interference from the free metal ions. Moreover, such complexes are unlikely to be useful *in vivo* because of this lability.

(34) Martell, A. E.; Smith, R. A. *Critical Stability Constants*; Plenum: New York, 1974; Vol. 1, p 332.
(35) Douhéret, G. *Bull. Soc. Chim. Fr.* **1965**, 5365−5372.
(36) Martin, R. B. *Met. Ions Biol. Syst.* **1979**, *9*, 1−39.
(37) Wilson, E. W.; Kasperian, M. H.; Martin, R. B. *J. Am. Chem. Soc.* **1970**, *92*, 5365−5372.
(38) Martin, R. B. *Met. Ions Biol. Syst.* **1974**, *1*, 129−156.
(39) Tsangaris, J. M.; Martin, R. B. *J. Am. Chem. Soc.* **1970**, *92*, 4255−4260.
(40) Pecoraro, V. L.; Rawlings, J.; Cleland, W. W. *Biochemistry* **1984**, *23*, 153−158.

Experimental Section.

Materials. Peptides and precursors and other chemicals were obained from commercial suppliers and used without purification. Porcine pancreatic α-amylase (EC 3.2.1.1, type I-A; PMSF treated, 2× crystallized suspension in 2.9 M NaCl solution containing 3 mM $CaCl_2$) was obtained from Sigma; *p*-nitrophenyl maltotrioside (*p*-NPG_3) was obtained from Böhringer Mannheim. Piperidine was distilled from CaH_2 before use, and solvents for HPLC were filtered through a 0.2-μm nylon filter. NMR spectra were obtained in CD_3OD and are referenced to CHD_2OD at 3.30 ppm for ^1H and CD_3OD at 49.0 ppm for ^{13}C.

Peptide Synthesis. The peptides were prepared using standard solid phase techniques with N^{α}-Fmoc protected amino acids on an N^{α}-Fmoc-O-^{t}Bu-tyrosine-Wang resin (Bachem California or Novabiochem). The ornithine and arginine side chains were protected with Boc and pmc, respectively. A typical experiment was carried out with 1 g of resin in a 100-mL vessel. Completion of each N-terminal deprotection and peptide bond formation was checked by the Kaiser ninhydrin test. The N-terminal Fmoc was removed with 20% piperidine in DMF prior to cleavage of the peptide from the resin. Side chain deprotection and cleavage from the resin were accomplished by treatment with the King mixture (0.75 g of crystalline phenol, 0.25 mL of ethylenedithiol, 0.5 mL of thioanisole, 0.5 mL of H_2O, and 10 mL of TFA) for 2 h. The resin was removed by filtration and washed with water (5 mL). The combined filtrate was treated with 250 mL of ether and the precipitate was collected and extracted with 50% acetonitrile/50% water (with 0.1% TFA). Solvent evaporation on a rotary evaporator followed by lyophilization gave the crude peptide, which was purified by preparative reverse-phase HPLC on a Vydac C18 column with a linear gradient of 0.1% TFA in water to 0.1% TFA in 60% acetonitrile/40% water, followed by lyophilization. All peptides were obtained as white solids of >95% purity by HPLC.

Gly-Trp-Arg-D-Tyr. ^1H NMR δ 7.58 (d, 1, J = 7.8 Hz), 7.31 (d, 1, J = 8.0 Hz), 7.13 (s, 1), 7.10−6.98 (m, 4), 6.70 (d, 2, J = 8.4 Hz), 4.69 (dd, 1, J = 5.3, 8.4 Hz), 4.60 (dd, 1, J = 4.7, 9.4 Hz), 4.33 (dd, 1, J = 5.4, 8.4 Hz), 3.72 (d, 1, J = 16.1 Hz), 3.59 (d, 1, J = 16.1 Hz), 3.26 (dd, 1, J = 5.3, 15.0 Hz), 3.16−2.95 (m, 4), 2.84 (dd, 1, J = 9.5, 14.0 Hz), 1.64 (m, 1), 1.44 (m, 1), 1.33−1.25 (m, 2). $^{13}C\{^1H\}$ NMR δ 174.9, 173.8, 173.0, 167.7, 158.6, 157.3, 138.1, 131.4, 129.0, 128.7, 124.8, 122.5, 119.9, 119.3, 116.3, 112.4, 110.4, 56.3, 55.3, 53.8, 42.0, 41.5, 37.8, 30.1, 28.9, 25.8. HRMS (FAB^+) calcd for $C_{28}H_{37}N_8O_6$ m/z 581.2836, found 581.2840.

Gly-Trp-Arg-Tyr. ^1H NMR δ 7.60 (d, 1, J = 7.9 Hz), 7.31 (d, 1, J = 8.1 Hz), 7.09−6.97 (m, 5), 6.70 (d, 2, J = 8.4 Hz), 4.72 (dd, 1, J = 5.5, 8.4 Hz), 4.55 (dd, 1, J = 5.2, 8.2 Hz), 4.35 (t, 1, J = 6.9 Hz), 3.69 (d, 1, J = 16.1 Hz), 3.55 (d, 1, J = 16.1 Hz), 3.25 (m, 1), 3.13−3.05 (m, 4), 2.89 (m, 1), 1.75 (m, 1), 1.63−1.51 (m, 3). $^{13}C\{^1H\}$ NMR δ 174.8, 173.8, 173.3, 167.3, 158.6, 157.4, 138.1, 131.4, 128.9, 128.7, 124.8, 122.5, 119.9, 119.3, 116.3, 112.4, 110.6, 55.9, 55.5, 54.0, 42.0, 41.5, 37.6, 30.3, 29.1, 25.9. HRMS (FAB^+) calcd for $C_{28}H_{37}N_8O_6$ m/z 581.2836, found 581.2823.

Gly-Trp-Orn-Tyr. ^1H NMR δ 7.60 (d, 1, J = 7.9 Hz), 7.32 (d, 1, J = 8.1 Hz), 7.10−6.97 (m, 5), 6.70 (d, 2, J = 8.5 Hz), 4.70 (dd, 1, J = 5.5, 8.4 Hz), 4.56 (dd, 1, J = 5.2, 8.1 Hz), 4.38 (t, 1, J = 6.6 Hz), 3.69 (d, 1, J = 16.1 Hz), 3.57 (d, 1, J = 16.1 Hz), 3.25 (m, 1), 3.13−3.06 (m, 2), 2.92−2.85 (m, 3), 1.81 (m, 1), 1.66−1.61 (m, 3). $^{13}C\{^1H\}$ NMR δ 174.7, 173.7, 173.0, 167.4, 157.4, 138.1, 131.4, 128.8, 128.7, 124.8, 122.5, 119.9, 119.3, 116.3, 112.4, 110.5, 55.9, 55.4, 53.6, 41.4, 40.2, 37.5, 30.0, 29.1, 24.7. HRMS (FAB^+) calcd for $C_{27}H_{35}N_6O_6$ m/z 539.2618, found 539.2613.

Trp-Arg-Tyr-Gly. ^1H NMR δ 7.64 (d, 1, J = 7.9 Hz), 7.37 (d, 1, J = 8.2 Hz), 7.14−6.98 (m, 5), 6.70 (d, 2, J = 8.4 Hz), 4.61 (dd, 1, J = 5.8, 8.6 Hz), 4.37 (t, 1, J = 6.7 Hz), 4.17 (dd, 1, J = 5.7, 8.4 Hz), 3.88 (s, 2), 3.39 (m, 1), 3.19−3.05 (m, 4), 2.83 (m, 1), 1.81−1.66 (m, 2), 1.56 (m, 2). $^{13}C\{^1H\}$ NMR δ 173.9, 172.8, 170.2, 158.7, 157.3, 138.3, 131.4, 128.9, 128.3, 125.8, 122.9, 120.3, 119.1, 116.3, 112.6, 107.9, 56.1, 54.7, 54.5, 42.0, 38.1, 30.4, 28.8, 25.8. HRMS (FAB^+) calcd for $C_{28}H_{37}N_8O_6$ m/z 581.2836, found 581.2829.

Enzyme Assays. Solutions were prepared using doubly distilled water and filtered through a 0.45-μm nylon filter. Assays were performed at 30 °C using a Kontron Uvikon 860 UV−vis spectrophotometer to measure the rate of hydrolysis of *p*-NPG_3 as substrate at 405 nm (ϵ = 9200 M^{-1} cm^{-1}). Enzyme dilutions were made with buffer containing 50 mM HEPES (pH 7.0), 60 mM NaCl, 2 mM $CaCl_2$, and 0.1 mg/mL BSA. The assay mixture contained 25 mM HEPES (pH 7.0), 30 mM NaCl, and 1 mM $CaCl_2$ in a total volume of 1.00 mL. Typically, 50 nM α-amylase was used and the sample was equilibrated for 5 min at 30 °C prior to initiation of the reaction with *p*-NPG_3.

Six substrate concentrations were used (0.25, 0.40, 0.50, 0.75, 1.0, 3.0 mM) with several independent determinations carried out at each concentration to determine K_m. For K_i measurements, 1.0 mM substrate was used. After substrate addition, 30 absorption points were recorded in a 10-min period, at which point the reaction was 5−10% complete. Good zero-order kinetics were observed. Initial rates and K_m values were calculated using the Enzfitter program, and K_i values were calculated by a Dixon analysis as well as other methods, using equations described in the above.

Acknowledgment. This work was supported by Grant No. GM30759 from the National Institutes of Health. We thank Dr. Peter Johann of Böhringer-Mannheim for providing a sample of *p*-nitrophenyl maltotrioside.

Supporting Information Available: Kinetic plots not shown above, and full derivation of eqs 10, 19, and 23 (8 pages). This material is contained in many libraries on microfiche, immediately follows this article in the microfilm version of the journal, can be ordered from the ACS, and can be downloaded from the Internet; see any current masthead page for ordering information and Internet access instructions.

JA952475+